J. Vorberger and D.O. Gericke, Physics of Plasmas **16**, 082702 (2009)

Coupled mode effects on energy transfer in weakly coupled, two-temperature plasmas

J. Vorberger and D.O. Gericke

Centre for Fusion, Space and Astrophysics,

Department of Physics, University of Warwick,

Coventry CV4 7AL, United Kingdom

(Dated: August 27, 2009)

Abstract

We investigate the effects of collective modes on the temperature relaxation in fully ionized, weakly coupled plasmas. A coupled mode (CM) formula for the electron-ion energy transfer is derived within the random phase approximation and we show how it can be evaluated using standard methods. The CM rates are considerably smaller than rates based on Fermi's Golden Rule for some parameters and identical for others. We show how the CM effects are connected to the occurrence of ion acoustic modes and when they occur. Interestingly, CM effects occur also for plasmas with very high electron temperatures; a regime, where the Landau-Spitzer approach is believed to be accurate.

PACS numbers: 52.25.Dg, 52.25.Kn, 52.27.Gr

I. INTRODUCTION

Sophisticated techniques to create and probe states with high energy density make it nowadays possible to test theories for dense plasmas. Properties investigated include the equation of state [1–3], collective phenomena [4], phase transitions [5–7], and the ion structure [8, 9]. As large and fast energy inputs are required, states far from equilibrium are created. The subsequent relaxation reveals many information on dynamic processes hidden or hard to probe in equilibrium. New ultra-fast x-ray sources [6, 10] make it possible to directly probe such states on a 10 ps time scale which overlaps with the time scale of temperature equilibration in dense plasmas.

However, the duration of temperature equilibration is still under discussion: the seminal Landau-Spitzer (LS) approach [11, 12] and early simulation results [13] were seriously questioned when a theory including coupled electron-ion modes found considerably longer relaxation times [14]. Strong indications for longer relaxations in dense plasmas were also found experimentally [15–17]. Classical collisions used in the LS approach may be the source for the deviations. However, a quantum approach for binary collisions yields even larger rates [18, 19] and, thus, increasing deviations from the CM theory.

Besides, relaxation is often rather complex and involves the interplay of all terms in the internal energy. Changing correlation and exchange energies [20, 21] and ionization kinetics including excitations [22–24] have been shown to considerable influence the equilibrium process.

Here, we focus on the electron-ion energy transfer in fully ionized, weakly coupled plasmas (see Refs. [25–28] for recent discussion on CM effects). In this limit, we can employ the well-established and well-tested random phase approximation (RPA) for the dynamic response functions and the Lenard-Balescu equation [29, 30] for a kinetic description. We use the quantum versions [31] of both to avoid ambiguities with respect to *ad hoc* cutoffs. On this basis, we derive a weak coupling version of the CM formula published by Dharma-wardana & Perrot [14]. We also obtain a form that can be evaluated by standard integration procedures.

Under certain conditions including systems with high electron temperatures, the CM theory predicts energy transfer rates that are about a factor of two lower than LS and FGR rates. These deviations are connected to the occurrence of ion acoustic modes and the related redistribution of weight in the dynamic response which also explains why the simpler

FGR formula agrees for other parameters. Based on well-established approximations, the results may serve as a benchmark. In particular, molecular dynamics simulations relying on classical mechanics and electron-ion pseudopotentials, applied e.g. in Refs. [32–34], can be tested against our analytic results.

II. ENERGY TRANSFER RATES

In ideal plasmas, electron-ion energy transfer rates are given by changes of the kinetic energy of species a via the one-particle Wigner distribution f_a

$$\frac{\partial}{\partial t}E_a = \int \frac{d\boldsymbol{p}}{(2\pi\hbar)^3}\,\frac{p^2}{2m_a}\,\frac{\partial}{\partial t}f_a(\boldsymbol{p},t)\,. \tag{1}$$

Using a general kinetic equation for homogeneous and isotropic systems, i.e., $\partial f_a/\partial t = \sum_b I_{ab}$, the energy transfer rates are determined by the type of the collision integral used. The equations for electrons and ions couple via $I_{ei} = I_{ie}$ and, thus, total energy is conserved.

There exists a hierarchy of kinetic equations [31] which can be divided into two classes: the first considers only binary collisions (Landau [11] and Boltzmann equations [35]); the second also includes collective effects (Lenard-Balescu-like equation [29, 30]). In the second kind, the mutual influence of electrons and ions is included via the common dielectric function and predicted to strongly modify the electron-ion energy transfer rates [14, 25].

The simplest approach for two-particle interactions considers classical binary collisions. The corresponding energy transfer rates are given by [11, 12]

$$\frac{\partial}{\partial t}E^{LS}_{e\to i} = \frac{3}{2}n_e k_B \frac{T_i - T_e}{\tau_{ei}} \tag{2}$$

with the electron-ion relaxation time

$$\tau_{ei} = \frac{3m_e m_i}{8\sqrt{2}n_i Z_i^2 e^4 \ln\Lambda}\left(\frac{k_B T_e}{m_e} + \frac{k_B T_i}{m_i}\right)^{3/2}\,. \tag{3}$$

The Coulomb logarithm is used here in the form [18] $\ln\Lambda = 0.5\ln(1+\lambda_e^2/(\varrho_\perp^2+\lambda_{dB}^2))$ with the screening length of electrons $\lambda_e = (k_B T_e/4\pi e^2 n_e)^{1/2}$, the distance of closest approach $\varrho_\perp = Z_i e^2/m_e v_{th}^2$, the deBroglie wave length $\lambda_{dB} = \hbar/m_e v_{th}$, and the thermal velocity $v_{th} = (k_B T_e/m_e)^{1/2}$. This form, which follows by considering hyperbolic orbits of the electrons, has the advantage to give non-negative results even for the dense plasmas.

The problems associated with classical collisions can be overcome within a quantum description that uses cross sections calculated from the two-particle Schrödinger equation

[18]. Interestingly, this yields rates for dense plasmas that are larger than the LS approach predicts.

The collective response of weakly coupled plasmas is described by the random phase approximation (RPA) given a dielectric function $\varepsilon^{RPA} = 1 - \sum_a V_{aa}\,\chi^0_{aa}$, where χ^0_{aa} are the density response functions of noninteracting systems. As the mutual influence of the electrons and ions is naturally included, the modes are fully coupled.

The kinetic equation corresponding to the RPA is the Lenard-Balescu equation [29, 30]. Using it in the energy balance (1) yields (see App. A for the derivation)

$$\frac{\partial}{\partial t} E^{CM}_{e\to i} = -4\hbar \sum_i \int \frac{d\boldsymbol{k}}{(2\pi\hbar)^3} \int_0^\infty \frac{d\omega}{2\pi}\, \omega \left| \frac{\mathrm{V}_{ei}(k)}{\varepsilon^{RPA}(k,\omega)} \right|^2 \times \operatorname{Im}\chi^0_{ee}(k\omega)\, \operatorname{Im}\chi^0_{ii}(k\omega)\, \Delta N_B(\omega)\,, \tag{4}$$

where $V_{ei}(k) = 4\pi Z e^2/k^2$ is the pure Coulomb potential and $\Delta N_B(\omega) = n^e_B(\omega) - n^i_B(\omega)$ is the difference of the occupation numbers of electron and ion modes, i.e. the Bose function $n^a_B(\omega) = [\exp(\hbar\omega/k_B T_a) - 1]^{-1}$. For all degrees of degeneracy, Eq. (4) is applicable for weakly coupled plasmas where it is equivalent to the expression derived by Dharma-wardana & Perrot [14] (see App. B). As the RPA describes coupled electron-ion systems, the zeros of $\varepsilon(k,\omega)$ define coupled modes (thus, 'CM' as label).

Fermi's golden rule (FGR) yields a more approximate model for the electron-ion energy transfer. Here, the species are treated independently and, thus, have distinct dielectric functions $\varepsilon^{RPA}_a = 1 - V_{aa}\,\chi^0_{aa}$. Accordingly, the expression for the energy transfer rates has a product of these dielectric functions in the denominator [14, 36]

$$\frac{\partial}{\partial t} E^{FGR}_{e\to i} = -4\hbar \sum_i \int \frac{d\boldsymbol{k}}{(2\pi\hbar)^3} \int_0^\infty \frac{d\omega}{2\pi}\, \frac{\omega\, |\mathrm{V}_{ei}(k)|^2}{|\varepsilon_e(k,\omega)|^2\, |\varepsilon_i(k,\omega)|^2} \times \operatorname{Im}\chi^0_{ee}(k\omega)\, \operatorname{Im}\chi^0_{ii}(k\omega)\, \Delta N_B(\omega)\,, \tag{5}$$

In lowest order, the FGR rate reduces to Landau-Spitzer-like expressions, either with soft or hard cutoffs [36, 37].

Although the CM (4) and the FGR (5) expressions contain the effects of collective excitations, they describe quite different systems. To evaluate the corresponding differences is the main purpose of this paper.

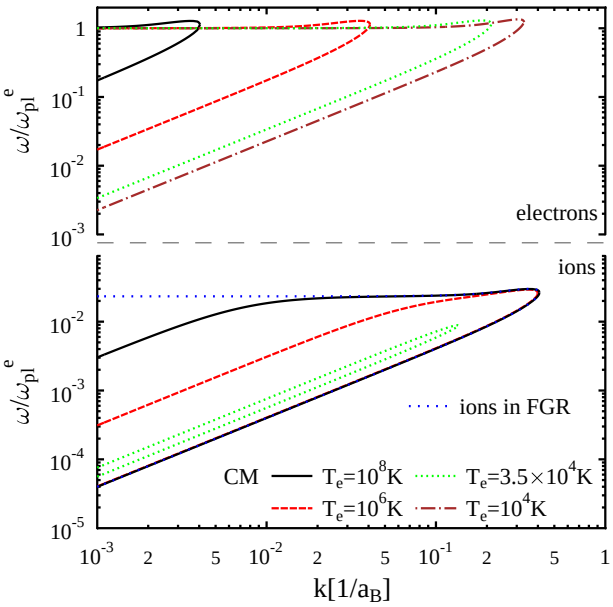

FIG. 1: (Color online) Dispersion relations, $\mathrm{Re}\varepsilon(k,\omega)=0$, for the collective modes in a hydrogen plasma with $n=10^{22}\,\mathrm{cm}^{-3}$, $T_i=10^4\,\mathrm{K}$, and different electron temperatures. In the FGR approach, an ion plasmon mode exists (upper dotted line) whereas all ion modes become acoustic for coupled systems.

III. EVALUATION OF THE CM & FGR EXPRESSIONS

The occurrence of collective modes is connected with sharp peaks in ω space. Without further consideration, these peaks prohibit the evaluation of Eqs. (4) and (5) by standard integration routines. We will first show under which conditions these modes occur and then describe the numerical integration procedure.

For the important small k, the mode frequencies are in very good approximation given by the zeros of the real part of the dielectric function. If the electron-ion coupling is neglected, both species have the well-known acoustic and plasmon-like branches (see Fig. 1) which are just scaled by Z_a and m_a. While the acoustic branch is strongly damped, the plasmon results in a sharp peak in the density response function at the plasmon frequency $\omega_{pl}^a \approx (4\pi Z_a e^2 n_a/m_a)^{1/2}$. As the ω-integral is effectively limited to frequencies $\omega<\omega_{pl}^i$ by the term $\mathrm{Im}\,\chi_{ii}^0(k,\omega)$, the electron modes are unimportant here.

The ion modes used in the FGR are independent and have always a plasmon branch. For coupled systems, the situation is qualitatively different: electron screening turns the

ion plasmon into a weakly damped ion acoustic branch. Interestingly, this ion acoustic mode becomes more plasmon-like for larger temperature differences and momenta. For the important small k values, the modes are however acoustic for all finite electron temperatures.

Fig. 1 also clearly demonstrates that the ion modes in the coupled system cease to exist if $|T_e - T_i|$ becomes too small. The sum over species in the full dielectric function puts strict limits to the occurrence of ion modes; a fact that is crucial for the understanding of the CM effect on the energy relaxation. It is well-known that ion acoustic modes exist for $T_i \ll T_e$ [38]; a more precise analysis (see App. C) shows that either of the relations [39]

$$\begin{aligned} T_i &\leq 0.27 \cdot Z_i\, T_e \qquad \text{for} \quad n_e \Lambda_e^3 \ll 1 \,, \\ T_i &\leq 0.27 \cdot Z_i\, T_F \qquad \text{for} \quad n_e \Lambda_e^3 \gg 1 \end{aligned} \tag{6}$$

must hold to allow for ion acoustic modes in weakly coupled electron-ion systems ($n_e \Lambda_e^3 = n_e (2\pi\hbar^2/m_e k_B T_e)^{3/2}$ is the degeneracy parameter). The upper case is valid for nondegenerate electrons; the lower line holds for highly degenerate electrons, where the Fermi temperature, i.e. $T_F = \hbar^2 (3\pi^2 n_e)^{2/3}/2 m_e k_B$, sets the scale. Accordingly, sharp ion acoustic modes may also occur for $T_e < T_i$ if the electron density is high enough.

The sharp peaks related to the zeros of the dielectric function represent a challenge for numerical integration. The FGR formula (5) can nevertheless be integrated in a re-written form: the integral is split into an unproblematic part without modes and a part including the modes that can be evaluated using the f-sum rule [40].

Often an analytical evaluation using the low frequency limit of the electron response function and a linearization of the Bose functions is possible [36, 37]. For such cases, we find excellent agreement to our numerical treatment. Differences for dense plasmas with $T_i \gg T_e$ can be traced back to the break-down of the approximations used for the analytical description.

It is impossible to treat the CM integrand the same way as the electron and ion parts are not separable. We can however re-arrange the ω-integral in a better way by artificially decomposing the total dielectric function into electron and ion parts: $\varepsilon^{RPA} = 1 + (\varepsilon_e - 1) + (\varepsilon_i - 1)$. Then we use $\operatorname{Im} \varepsilon_a^{RPA}(k,\omega) = V_{aa}(k) \operatorname{Im} \chi_{aa}^0(k,\omega)$ to express the density response functions $\chi_{aa}^0(k,\omega)$ in terms of dielectric functions. For fully ionized plasmas, $V_{ei}^2 = V_{ii} V_{ee}$ holds and

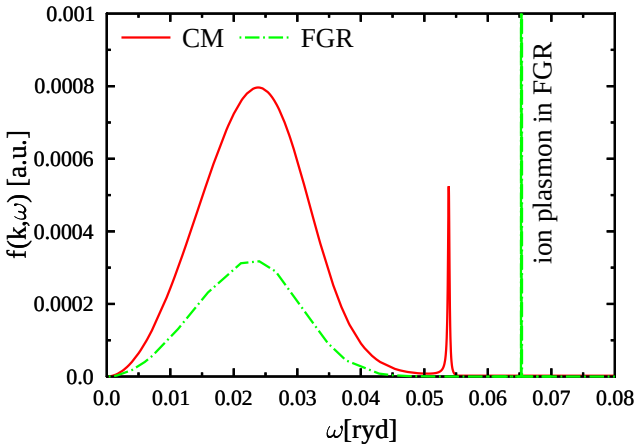

FIG. 2: (Color online) Combination of dielectric functions in the CM and FGR expressions, i.e. $f^{\rm CM} = {\rm Im}\varepsilon_e {\rm Im}\varepsilon_i/|\varepsilon|^2$ and $f^{\rm FGR} = {\rm Im}\varepsilon_e {\rm Im}\varepsilon_i/|\varepsilon_e|^2|\varepsilon_i|^2$, respectively. Considered is a small wave number of $k = a_B^{-1}$ and a hydrogen plasma with $T_i = 10^5\,{\rm K}$, $T_e = 10^6\,{\rm K}$, and $n = 10^{24}\,{\rm cm}^{-3}$. Note: the height of the ion plasmon peak in the FGR approach is 1500 a.u.

the ω-integral is transformed into

$$I_\omega = \int_0^\infty \frac{d\omega}{2\pi}\,\omega\,\Delta N_{ei}(\omega)\frac{{\rm Im}\,\varepsilon_e(k,\omega)\;{\rm Im}\,\varepsilon_i(k\omega)}{|\varepsilon^{RPA}(k,\omega)|^2}\,. \tag{7}$$

This form can still have sharp peaks at the positions of the ion acoustic modes, but these peaks are limited since

$$\lim_{{\rm Re}\,\varepsilon\to 0}\frac{{\rm Im}\,\varepsilon_e(k,\omega)\;{\rm Im}\,\varepsilon_i(k,\omega)}{|\varepsilon^{RPA}(k,\omega)|^2} = \frac{{\rm Im}\,\varepsilon_e(k,\omega)\;{\rm Im}\,\varepsilon_i(k,\omega)}{|{\rm Im}\,\varepsilon_e(k,\omega)+{\rm Im}\,\varepsilon_i(k,\omega)|^2} < 1\,. \tag{8}$$

Thus, this rearrangement makes a brute force approach for integrating the CM equation (7) feasible.

Examples for the ω-integrand for the two approaches are plotted in Fig. 2 for a wave number small enough for the ion acoustic mode to exists. Clearly, the acoustic mode is shifted to the left and has a strongly reduced height. Although the particle excitation (left broad peak) is increased, it cannot compensate the loss in weight. For a pure ion system (FGR), almost the entire weight stems from the plasmon peak whereas the main contribution to the CM integral comes from the particle peak.

The difference in mode structure are the basics for the CM effects. Figure 3 demonstrates that CM effects are caused by small k where the ion acoustic mode exists. These modes are

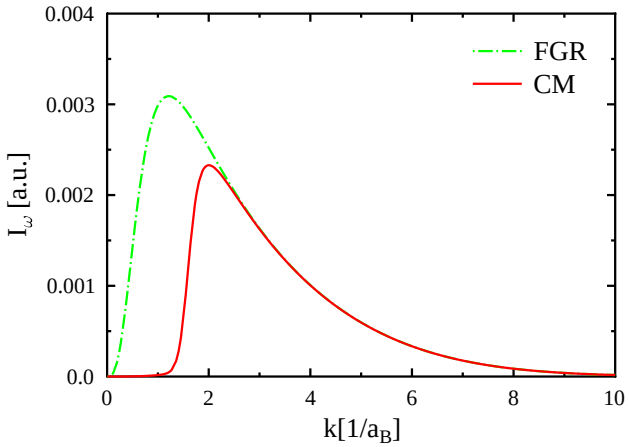

FIG. 3: (Color online) Examples for the ω-integral in the CM and FGR expressions for hydrogen as in Fig. 2.

shifted and reduced in weight; their contributions to the CM integral are of the same order as the particle peak of the FGR (see Fig. 2) which, in turn, is negligible compared to the ion plasmon peak. Thus, small k give almost no contribution in the CM expression compared to the FGR and the CM rates can be significantly reduced if these small k are important. For large k, neither the ion acoustic nor the ion plasmon mode exists and the CM and FGR ω-integrals merge.

IV. RESULTS AND DISCUSSION OF THE ENERGY TRANSFER RATES

Based on the methods presented above, we can directly evaluate the CM and FGR expressions (4) and (5). In a first example, high-density hydrogen with $T_e > T_i$ is considered in Fig. 4. All approaches yield similar curves: increasing rates when electron and ion temperatures are comparable, followed by a maximum, and finally a LS-like asymptotic reduction of the rates $\sim T_e^{1/2}$. However, considerable quantitative differences arise between the approximation levels presented.

If $T_e \approx T_i$, the FGR and CM results agree since ion acoustic modes do not exist. The LS rates differ as the Coulomb logarithm is not well defined for dense plasmas with degenerate electrons. At about $T_e = 10^6$ K, ion acoustic modes start to occur and the CM results show increasing deviations from the FGR rates. Around $T_e = 10^7$ K, ion acoustic modes are fully developed. Since they reduce the ω-integral for small k (see Fig. 3), the CM rates show

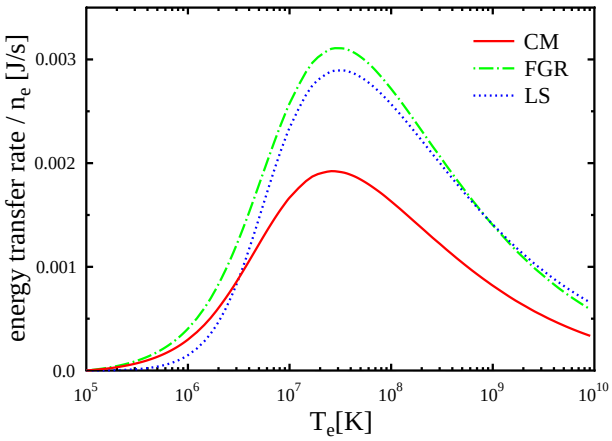

FIG. 4: (Color online) Energy transfer rates in fully ionized hydrogen with $n = 10^{26}\,\mathrm{cm}^{-3}$ and $T_i = 10^5\,\mathrm{K}$. Curves follow from the CM (4), FGR (5), and LS (2) expressions.

here a considerable lowering. For high electron temperatures, the LS formula is believed to be applicable. However, our results show that only LS and FGR rates agree in this limit. The CM formula (4) yields here a considerably reduced energy transfer making CM effects important for hot fusion plasmas. They only cease to exist for hot ions where no ion acoustic modes exist.

The relation between the CM and FGR approaches is studied in Fig. 5 in more detail. The upper panel shows how increasing densities enhance the lowering of the CM energy transfer rates. Whereas CM effects slowly develop with temperature difference for the lower densities, they are already present at $T_e = T_i$ for densities above $n = 10^{23}\,\mathrm{cm}^{-3}$. Here, the electrons are degenerate with $T_F > T_i$ and ion acoustic modes occur independent of T_e. An extreme case is given for $n = 10^{26}\,\mathrm{cm}^{-3}$ where a lowering of CM rates of up to 90% can be found.

The effect of the ion temperatures is illustrated in the lower panel of Fig. 5. CM effects are well established for $T_i = 10^4 K$, but vanish for higher ion temperatures. Nevertheless, sufficiently hot electrons always guarantee lower CM rates. Interestingly, the ratio of CM and FGR rates approaches 1/2 for very high electron temperatures.

Let us analyze the high temperature, low density limit of the CM energy transfer rate in more detail (see Fig. 6). The CM and FGR approaches do agree in the weak coupling limit *if and only if* the temperature difference between the subsystems is sufficiently low so that no coupled collective modes can be excited. Larger deviations occur for increased temperature

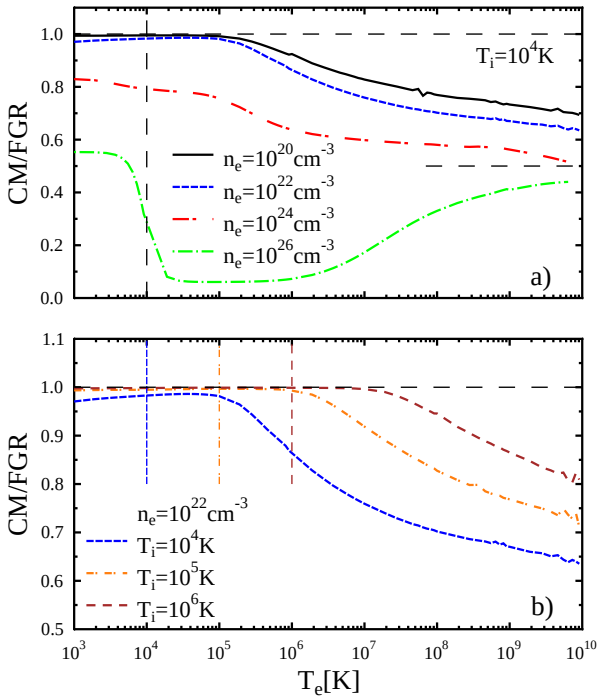

FIG. 5: (Color online) Ratio of the CM and FGR energy transfer rates for fully ionized hydrogen as a function of the electron temperature. Panel a) considers various densities while the ion temperature is constant; panel b) shows results for different ion temperatures at constant density. All results are obtained within the random phase approximation. The vertical lines mark the condition $T_e = T_i$.

differences and smaller electron temperatures (more strongly coupled ions; although RPA is used in Fig. 6). However, even for very large electron temperatures the CM effects still reduce the coupling between the electron and ion components.

Moreover, FGR and LS have a ratio independent of the temperature difference. In addition, numerics show, that even in the weakly coupled case with small temperature difference, FGR and LS curves intersect rather than converge. This is due to the poor cut off in the Coulomb integral in LS. Thus, the FGR approach rather than LS formula should be used to compare with experiments or simulations if one searches for coupled mode effects in the data.

Coupled mode effects are of course more pronounced for higher ion charge states since here ion acoustic modes already occur for smaller temperature differences (see condition (6)) and also exist for larger k values. Fig. 7 shows an example. Energy transfer rates normal-

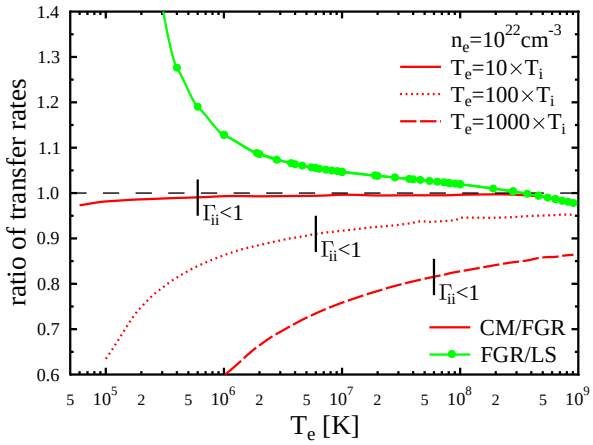

FIG. 6: (Color online) Ratio of energy transfer rates in CM, FGR, and LS in the high temperature (low coupling) limit for fully ionized hydrogen. Curves for different ratios of electron and ion temperature are given. The three curves below unity belong to the ratio of CM to FGR rate. The ratio of FGR rate and LS rate is independent of the temperature ratio and is given by the green dotted line. The region were the ion coupling is small is indicated for each case.

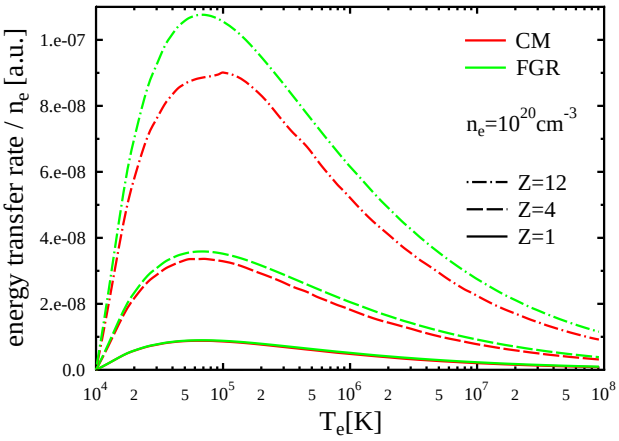

FIG. 7: (Color online) Effect of the (nonequilibrium) ion charge state on the energy transfer rates for $T_i = 10^4 K$.

ized to the electron density rise linearly with the charge Z_i in FGR, but we find stronger reductions due to coupled electron-ion modes for higher Z_i. Particularly for smaller electron temperatures, CM effects are more pronounced for more highly charged ions as ion acoustic modes might not exist for lower charges. Different ion masses are, on the other hand, irrelevant as the give similar scaling in the CM and FGR expressions.

V. SUMMARY AND CONCLUSIONS

We have investigated the electron-ion energy transfer rates in two-temperature plasmas with special emphasis on coupled mode effects. For weakly coupled plasmas, we can rely on the random phase approximation to describe the modes in coupled electron-ion systems. It is shown that a coupled mode formula can be derived from the quantum version of the Lennard-Balescu equation without further approximations. This expression is accurate for weakly coupled plasmas of any degeneracy.

For certain conditions, the coupled mode expression yields considerably reduced electron-ion energy transfer when compared to the LS and FGR approaches. A detailed analysis showed that this reduction can be traced back to the presence of ion acoustic modes and a related redistribution of weight in the dielectric response function. Precise conditions for the occurrence of ion acoustic modes and the coupled mode reduction of the energy transfer rates were derived. Interestingly, the CM reduction is preserved for very high electron temperatures where the rates are roughly a factor of two lower than FGR or LS rates. An agreement between CM and FGR expressions can only be reached if the temperature difference is small or the ion temperature is sufficiently high to prohibit the occurrence of ion acoustic modes.

We gratefully acknowledge financial support from the Engineering and Physical Sciences Research Council and stimulating discussions with Prof. W.-D. Kraeft.

Appendix A: Derivation Coupled Mode Expression in RPA

The quantum Lennard-Balescu equation for electrons in homogeneous and isotropic plasmas reads [31]

$$\begin{aligned}\frac{\partial}{\partial t}f_e(p,t) = \frac{1}{\hbar}\sum_i \int \frac{d\boldsymbol{p}'}{(2\pi\hbar)^3}\frac{d\overline{\boldsymbol{p}}}{(2\pi\hbar)^3}\frac{d\overline{\boldsymbol{p}}'}{(2\pi\hbar)^3} \left|\frac{\mathrm{V}_{ei}(\boldsymbol{p}-\overline{\boldsymbol{p}})}{\varepsilon^{RPA}\left(\boldsymbol{p}-\overline{\boldsymbol{p}}, E_e(p)-E_e(\overline{p}),t\right)}\right|^2 \\ \times 2\pi\delta\left(E_e(\boldsymbol{p})+E_i(\boldsymbol{p}')-E_e(\overline{\boldsymbol{p}})-E_i(\overline{\boldsymbol{p}}')\right)(2\pi\hbar)^3\,\delta\Big(\boldsymbol{p}+\boldsymbol{p}'-\overline{\boldsymbol{p}}-\overline{\boldsymbol{p}}'\Big) \\ \times\Big\{f_e(\overline{\boldsymbol{p}},t)f_i(\overline{\boldsymbol{p}}',t)\left[1-f_e(\boldsymbol{p},t)\right]\left[1-f_i(\boldsymbol{p}',t)\right]-f_e(\boldsymbol{p},t)f_i(\boldsymbol{p}',t)\left[1-f_e(\overline{\boldsymbol{p}},t)\right]\left[1-f_i(\overline{\boldsymbol{p}}',t)\right]\Big\}.\end{aligned} \tag{A1}$$

The sum runs over all species, but only ions contribute to the energy relaxation. $E_a(p) = p^2/2m_a$ denotes the kinetic energy of particles of species a and $V_{ab}(k)$ is the Coulomb potential. Dynamic screening is included by the retarded dielectric function which is used in RPA $\varepsilon^{RPA}(\boldsymbol{p}, E, t) = 1 - \sum_a V_{aa}(p)\, \chi^0_{aa}(\boldsymbol{p}, E, t)$ and relates the dielectric function to the density response function of free particles. This density response is given by

$$\chi^0_{aa}(\boldsymbol{p}, E, t) = \int \frac{d\boldsymbol{p}'}{(2\pi\hbar)^3} \frac{f_a(\boldsymbol{p}', t) - f_a(\boldsymbol{p}' + \boldsymbol{p}, t)}{E + E_a(\boldsymbol{p}') - E_a(\boldsymbol{p}' + \boldsymbol{p}) + i\epsilon}\,, \tag{A2}$$

which is, in turn, determined by the electron or the ion distribution functions.

The electron-ion energy transfer rates are obtained by multiplying the Lenard-Balescu equation (A1) by the electron energy, $E_e = p^2/2m_e$, and an integration over the free momentum (see balance equation (1). For the further proceedings, it is useful to consider the transfer of momentum and energy during the collision, $\boldsymbol{k} = \boldsymbol{p} - \overline{\boldsymbol{p}}$ and $\omega = E_e(p) - E_e(\overline{p})$, respectively. With these new variables, one can now apply the relations between Fermi and Bose functions $n^a_B(\omega) = [\exp(\hbar\omega/k_B T_a) - 1]^{-1}$, namely

$$\begin{aligned} &f_a(\boldsymbol{p})\,[1 - f_a(\boldsymbol{p} + \boldsymbol{k})] = \\ &\qquad [f_a(\boldsymbol{p} + \boldsymbol{k}) - f_a(\boldsymbol{p})]\, n^a_B\Big(E_a(\boldsymbol{p}) - E_a(\boldsymbol{p} + \boldsymbol{k})\Big)\,, \end{aligned} \tag{A3}$$

The set of distributions in the third line of the collision integral of the Lenard-Balescu equation (A1) can then be written as

$$\begin{aligned} \Big\{f()\Big\} = &[f_e(\overline{\boldsymbol{p}} + \boldsymbol{k}) - f_e(\overline{\boldsymbol{p}})]\,[f_i(\boldsymbol{p}') - f_i(\boldsymbol{p}' + \boldsymbol{k})] \\ &\times \Big[n^e_B(-\omega)\, n^i_B(\omega) - n^e_B(\omega)\, n^i_B(-\omega)\Big]\,. \end{aligned} \tag{A4}$$

With these transformations, we obtain for the electron-ion energy transfer rate

$$\begin{aligned} \frac{\partial}{\partial t} E^{CM}_{e\to i} = &-\frac{1}{\hbar} \sum_i \int \frac{d\overline{\boldsymbol{p}}}{(2\pi\hbar)^3} \frac{d\boldsymbol{k}}{(2\pi\hbar)^3} \frac{d\omega}{2\pi}\; E_e(\overline{\boldsymbol{p}} + \boldsymbol{k}) \left|\frac{\mathrm{V}_{ei}(\boldsymbol{k})}{\varepsilon^R(\boldsymbol{k}\omega)}\right|^2 \\ &\times \Big[f_e(\overline{\boldsymbol{p}} + \boldsymbol{k}) - f_e(\overline{\boldsymbol{p}})\Big] 2\pi\delta\Big(\omega - E_e(\overline{\boldsymbol{p}} + \boldsymbol{k}) + E_e(\overline{\boldsymbol{p}})\Big) \\ &\times \Big[n^e_B(-\omega)\, n^i_B(\omega) - n^e_B(\omega)\, n^i_B(-\omega)\Big] \\ &\times \int \frac{d\boldsymbol{p}'}{(2\pi\hbar)^3}\, [f_i(\boldsymbol{p}') - f_i(\boldsymbol{p}' + \boldsymbol{k})]\; 2\pi\delta\Big(\omega - E_i(\boldsymbol{p}' + \boldsymbol{k}) + E_i(\overline{\boldsymbol{p}}')\Big)\,. \end{aligned} \tag{A5}$$

The integral in the second line is the imaginary part of the r.h.s. of Eq. (A2): $\mathrm{Im}\,\chi^0_{ii}(k\omega)$. The difference of Bose functions determines the direction of the energy transfer. After changing variables to $\omega'=-\omega$, $\boldsymbol{k}'=-\boldsymbol{k}$, $\boldsymbol{p}'=\overline{\boldsymbol{p}}-\boldsymbol{k}'$ in the second term proportional to $n^e_B(\omega)\,n^i_B(-\omega)$, this term has the same form as the first one, except that the energy in front of the screened potential is $E_e(\overline{\boldsymbol{p}})$ instead of $E_e(\overline{\boldsymbol{p}}-\boldsymbol{k})$. Applying the energy conserving δ-function in the collision integral yields $E_e(\overline{\boldsymbol{p}}+\boldsymbol{k})-E_e(\overline{\boldsymbol{p}})=\omega$.

Now the remaining electron distributions together with the energy conserving δ-function give also the definition of an imaginary part of the free density response function: $\mathrm{Im}\,\chi^0_{ee}(k\omega)$. The energy transfer rate is thus given by

$$\frac{\partial}{\partial t}E^{CM}_{e\to i} = -4\hbar\sum_i\int\frac{d\boldsymbol{k}}{(2\pi\hbar)^3}\int_{-\infty}^{\infty}\frac{d\omega}{2\pi}\,\omega\,\left|\frac{\mathrm{V}_{ei}(k)}{\varepsilon^{RPA}(k\omega)}\right|^2 \times \mathrm{Im}\,\chi^0_{ee}(k\omega)\;\mathrm{Im}\,\chi^0_{ii}(k\omega)\,n^e_B(-\omega)\,n^i_B(\omega)\,. \tag{A6}$$

If we use the fact that $[1/2-n_B(\omega)]$ and $\mathrm{Im}\,\chi^0_{aa}(\omega)$ are odd functions with respect to ω, we can rearrange the upper expression in the form

$$\frac{\partial}{\partial t}E^{CM}_{e\to i} = -4\hbar\sum_i\int\frac{d\boldsymbol{k}}{(2\pi\hbar)^3}\int_{0}^{\infty}\frac{d\omega}{2\pi}\;\omega\,\left|\frac{\mathrm{V}_{ei}(k)}{\varepsilon^{RPA}(k\omega)}\right|^2 \times \mathrm{Im}\,\chi^0_{ee}(k\omega)\;\mathrm{Im}\,\chi^0_{ii}(k\omega)\left[n^e_B(\omega)-n^i_B(\omega)\right]. \tag{A7}$$

This expression gives the electron-ion energy transfer rate in RPA including the effects of coupled collective modes.

Appendix B: Equivalence to Coupled Mode Expression Derived by Dharma-wardana & Perrot

The coupled mode expression derived by Dharma-wardana & Perrot, equation (50) in Ref. [14], reads

$$\dot{E}_{rlx} = \hbar\int_0^{\infty}\frac{d\omega}{2\pi}\int\frac{d\mathbf{k}}{(2\pi\hbar)^3}\,\omega\,V^2_{ie}(k)\;\Delta N_{ei}(\omega) \times\frac{A^i(k,\omega)\,A^e(k,\omega)}{|1-V^2_{ie}(k)\,\chi_{ee}(k,\omega)\,\chi_{ii}(k,\omega)|^2}\,, \tag{B1}$$

where we assumed all potentials to be of Coulomb type for simplicity. The difference of Bose functions is here the same as in Eq. (A7): $\Delta N_{ei} = n_B^e(\omega) - n_B^i(\omega)$. The functions $A^a(k,\omega)$ are given by

$$A^a(k,\omega) = -2\mathrm{Im}\chi_{aa}(k,\omega)\,. \tag{B2}$$

One should however notice that $\chi_{aa}(k,\omega)$ are full density response functions of a coupled system.

In RPA, these density response function can also be written in terms of the free particle response and the dielectric function of the (fully coupled) medium [42]

$$\chi_{aa}(k,\omega) = \frac{\chi^0_{aa}(k,\omega)}{1 - V_{aa}(k)\chi^0_{aa}(k,\omega)} = \frac{\chi^0_{aa}(k,\omega)}{\varepsilon_{aa}(k,\omega)}\,. \tag{B3}$$

The real and imaginary parts can then be expressed as

$$\mathrm{Re}\chi_{aa}(k,\omega) = \frac{\mathrm{Re}\varepsilon_a(k,\omega) - |\varepsilon_a(k,\omega)|^2}{V_{aa}(k)|\varepsilon_a(k,\omega)|^2}\,, \tag{B4}$$

$$\mathrm{Im}\chi_{aa}(k,\omega) = -\frac{\mathrm{Im}\varepsilon_a(k,\omega)}{V_{aa}(k)|\varepsilon_a(k,\omega)|^2}\,. \tag{B5}$$

With these relations, the denominator in Eq. (B1) which constitutes the differences to the FGR formula becomes

$$|1 - V_{ie}^2(k)\,\chi_{ee}(k,\omega)\chi_{ii}(k,\omega)|^2 = \frac{|\varepsilon(k,\omega)|^2}{|\varepsilon_e(k,\omega)|^2|\varepsilon_i(k,\omega)|^2}\,. \tag{B6}$$

The dielectric function in the nominator is the one for the full system. The partial dielectric functions ε_a in the denominator are cancelled by the one contained in the imaginary part of the density response functions χ_{aa} (see Eq. (B5)). Hence, one obtains an expression identical to Eq. (A7) by inserting these rearrangements into Eq. (B1).

Appendix C: Conditions for the Occurrence of Ion Acoustic Modes

For ion acoustic modes to exist, the real part of the total dielectric function must vanish. We can consider the ionic contribution in non-degenerate limit. In RPA, the real part of χ^0_{ii} can be written as [31, 42]

$$\mathrm{Re}\chi^0_{ii}(k,\omega) = \frac{n_i}{k_B T}\left[1 - \frac{\omega^2 m_i}{p^2 k_B T}\,{}_1F_1\left(1, \frac{3}{2}, -\frac{\omega^2 m_i}{2p^2 k_B T}\right)\right] \tag{C1}$$

with the confluent hypergeometric function which can be approximated by a Padé formula as follows [31]

$$ {}_1F_1(-x) = \frac{1 + \frac{x}{3} + \frac{x^2}{10} + \frac{x^3}{42} + \frac{x^4}{218} + \frac{7x^5+x^6}{9360}}{1 + x + \frac{x^2}{2} + \frac{x^3}{6} + \frac{x^4}{24} + \frac{x^5}{120} + \frac{x^6}{720} + \frac{x^7}{4860}} \,. \tag{C2} $$

For ion acoustic modes to occur, the minimum of the response functions (C1) must at least compensate the electronic contribution plus unity. We thus search for an approximation of Eq. (C2) that conserves the location of its minimum and find from the frequency derivative $\omega_0 \approx 2.36\, k\, (k_B T_i/m_i)^{1/2}$. Using ω_0 in Eq. (C1) yields

$$ \mathrm{Re}\, \varepsilon_i(k, \omega_0) = 1 - 0.27\, \frac{\kappa_i^2}{k^2} \,, \tag{C3} $$

where $\kappa_i = (4\pi Z_i^2 e^2 n_i / k_B T_i)^{1/2}$ is the inverse of the ion part of the classical Debye screening length.

For the electronic part, we can use the static long wave length limit $\mathrm{Re}\, \varepsilon_e(k, 0) = 1 + (\kappa_e/k)^2$. For small momenta, the unity can be neglected and we find the condition

$$ \kappa_e^2 \leq 0.27\, \kappa_i^2 \,. \tag{C4} $$

Eq. (C4) quantifies the known condition $T_i \ll T_e$ [38] for ion acoustic waves. Temperature relations may be obtained by inserting an appropriate expression for the electron screening length, i.e., either the classical Debye length or the Thomas-Fermi screening length.

---

[1] G.W. Collins *et al.*, Science **281**, 1178 (1998).

[2] M.D. Knudson *et al.*, Phys. Rev. Lett. **87**, 225501 (2001).

[3] R.F. Smith *et al.*, Phys. Rev. Lett. **98**, 065701 (2007).

[4] S.H. Glenzer *et al.*, Phys. Rev. Lett. **98**, 065002 (2007).

[5] V.E. Fortov *et al.*, Phys. Rev. Lett. **99**, 185001 (2007).

[6] A.L. Kritcher *et al.*, Science **322**, 69 (2008).

[7] A. Grinenko *et al.*, Phys. Rev. Lett. **101**, 194801 (2008).

[8] A. Ravasio *et al.*, Phys. Rev. Lett. **99**, 135006 (2007).

[9] E. Garćia Saiz *et al.*, Nature Physics **4**, 940 (2008).

[10] B. Barbrel *et al.*, Phys. Rev. Lett **102**, 165004 (2009).

[11] L.D. Landau, Phys. Z. Sowjetunion **10** 154 (1936).

[12] L. Spitzer, *Physics of Fully Ionized Gases*

[13] J.P. Hansen, I.R. McDonald, Phys. Lett. A **97**, 42 (1983).

[14] M.W.C. Dharma-wardana and F. Perrot, Phys. Rev. E **58**, 3705 (1998).

[15] D. Riley *et al.*, Phys. Rev. Lett. **84**, 1704 (2000).

[16] P. Celliers *et al.*, Phys. Rev. Lett. **68**, 2305 (1992).

[17] A. Ng *et al.*, Phys. Rev. E **52**, 4299 (1995).

[18] D.O. Gericke, M.S. Murillo, and M. Schlanges, Phys. Rev. E **65**, 036418 (2002).

[19] Note that the use of classical collision theory yields, for increasing density, first too low than negative Coulomb logarithms and energy transfer rates.

[20] D.O. Gericke *et al.*, J. Phys. A **36**, 6087 (2003).

[21] D.O. Gericke, Th. Bornath, and M. Schlanges, J. Phys. A **39**, 4739 (2006).

[22] Th. Ohde *et al.*, Phys. Plasmas **3**, 1241 (1996).

[23] Th. Bornath, M. Schlanges, and R. Prenzel, Phys. Plasmas **5**, 1485 (1998).

[24] D.O. Gericke *et al.*, J. Phys. A **39**, 4727 (2006).

[25] M.W.C. Dharma-wardana, Phys. Rev. E **64**, 035401(R) (2001).

[26] J. Daligault and D. Mozyrsky, Phys. Rev. E **75**, 026402 (2007).

[27] J. Daligault and D. Mozyrsky, High Energy Density Physics **4**, 58 (2008).

[28] G. Gregori and D.O. Gericke, Europhys. Lett. **83**, 15002 (2008).

[29] A. Lenard, Ann. Phys. **3**, 390 (1960).

[30] R. Balescu, Phys. Fluids **3**, 52 (1960).

[31] D. Kremp, M. Schlanges, and W.-D. Kraeft, *Quantum Statistics of Nonideal Plasmas* (Springer, Berlin, 2006).

[32] G. Dimonte and J. Daligault, Phys. Rev. Lett. **101**, 135001 (2008).

[33] J.N. Glosli *et al.*, Phys. Rev. E **78**, 025401(R) (2008).

[34] B. Jeon *et al.*, Phys. Rev. E **78**, 036403 (2008).

[35] P. Danielewicz, Ann. Phys. (N.Y.) **152** 239 (1984).

[36] D.O. Gericke, J. Phys. (Conf. Series) **11**, 111 (2005).

[37] G. Hazak *et al.*, Phys. Rev. E **64**, 066411 (2001).

[38] L.D. Landau and E.M. Lifshitz, *Course in Theoretical*

Physics (Pergamon, Oxford, 1981).

[39] J. Vorberger and D.O. Gericke, J. Phys. (Conf. Series) **112**, 032077 (2008).

[40] W.-D. Kraeft, B. Strege, and M. Girardeau, Contrib. Plasma Phys. **30**, 563 (1990).

[41] H. Brysk, Plasma Phys. **16**, 927 (1974).

[42] W.-D. Kraeft, D. Kremp, W. Ebeling, and G. Röpke, *Quantum Statistics of Charged Particle Systems*

(Akademie-Verlag, Berlin, 1986).

[43] M.W.C. Dharma-wardana, Phys. Rev. Lett. **101**, 035002 (2008).